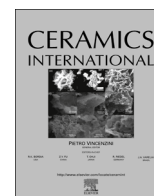




ELSEVIER

Contents lists available at ScienceDirect

Ceramics International

journal homepage: [www.elsevier.com/locate/ceramint](http://www.elsevier.com/locate/ceramint)

# Magnetic properties of $\text{Co}_3\text{O}_4$ polycrystal powder

Z. Seidov<sup>a</sup>, M. Açıkgöz<sup>b,\*</sup>, S. Kazan<sup>c</sup>, F. Mikailzade<sup>a,c</sup>

<sup>a</sup> Institute of Physics, Azerbaijan National Academy of Sciences, AZ – 1143 Baku, Azerbaijan

<sup>b</sup> Bahcesehir University, Faculty of Engineering and Natural Sciences, Beşiktaş, 34353 Istanbul, Turkey

<sup>c</sup> Department of Physics, Gebze Technical University, Gebze 41400, Kocaeli, Turkey

## ARTICLE INFO

### Article history:

Received 4 February 2016

Received in revised form

9 May 2016

Accepted 10 May 2016

Available online 11 May 2016

### Keywords:

$\text{Co}_3\text{O}_4$

Antiferromagnetism

ESR

Powder

## ABSTRACT

The results of investigations of magnetic properties of  $\text{Co}_3\text{O}_4$  polycrystals in powder morphology with average crystallite size of  $10\ \mu\text{m}$  are presented. The temperature dependence of the magnetic susceptibility, measured in a wide temperature interval ( $1.5 \leq T \leq 400\ \text{K}$ ) using SQUID magnetometer, as well as electron spin resonance (ESR) spectra measured at X-band and Q-band frequency ranges have been studied. Antiferromagnetism with a Néel temperature  $T_N$  at about 39 K was observed from the analysis of evolution of molar magnetic susceptibility and ESR intensity as a function of temperature. ESR parameters namely g-factor, intensity ( $I_{\text{ESR}}$ ), g-value, and linewidth  $\Delta H$  for powder  $\text{Co}_3\text{O}_4$  have been obtained. Some deviations from the expected values of some magnetic properties were determined and discussed.

© 2016 Elsevier Ltd and Techna Group S.r.l. All rights reserved.

## 1. Introduction

In recent years there is a growing interest in investigations of magnetic, optical, physical and transport properties of transition metal oxide  $\text{Co}_3\text{O}_4$ , which is an attractive and promising material due to its extensive applications in data storage, gas sensing, catalysts and electrochemical devices [1–6].  $\text{Co}_3\text{O}_4$  is a magnetic p-type semiconductor and belongs to the group of crystals having the normal spinel crystal structure with a formula  $\text{ABO}_4$ , where in cubic phase A and B represent the tetrahedral sites occupied by  $\text{Co}^{2+}$  ( $S=3/2$ ) ions and octahedral sites occupied by  $\text{Co}^{3+}$  ( $S=0$ ) ions, respectively. They are localized inside a cubic close packing array of oxide ions, where the  $32\ \text{O}^{2-}$  ions occupy  $32(e)$  sites [7]. The crystal structure and illustrations of the tetrahedral  $[\text{Co}^{2+}\text{O}_4]$  and octahedral  $[\text{Co}^{3+}\text{O}_6]$  are depicted in Fig. 1. It was recently reported that  $\text{Co}_3\text{O}_4$  undergoes a first-order transition from a cubic  $Fd\bar{3}m$  to a lower-symmetry monoclinic  $P2_1/c$  phase at 35 GPa, due to the local high-spin to low-spin phase transition [8]. Furthermore, it was demonstrated that the tetrahedral  $\text{AO}_4$  and octahedral  $\text{BO}_6$  coordination of  $\text{Co}^{2+}$  and  $\text{Co}^{3+}$  in cubic phase, respectively, turn out to the octahedral  $\text{AO}_6$  and  $\text{BO}_6$  coordination of both  $\text{Co}^{2+}$  and  $\text{Co}^{3+}$  in the high-pressure phase. Most of its magnetic moment emerges from spins of  $\text{Co}^{2+}$  ions and also a small contribution comes from spin-orbit coupling [9]. It is known that cubic phase of  $\text{Co}_3\text{O}_4$  is an antiferromagnetic material ordering with the super-exchange interactions through the favorable path

$\text{Co}^{2+}-\text{O}-\text{Co}^{3+}-\text{O}-\text{Co}^{2+}$  as well as with the Neel temperature ( $T_N$ ) of about 40 K [9,10].

Recently much attention has been made to investigations of the magnetic properties of bulk and nanostructured  $\text{Co}_3\text{O}_4$  [11–16]. In this frame considerable research has been made by authors of [15], in which a comparative study of the magnetic and EPR parameters of bulk and nanoparticle  $\text{Co}_3\text{O}_4$  was presented. In this work the authors pointed to differences in magnetic properties of the samples in different morphologies. Additionally, there are a number of peculiarities of antiferromagnetic systems to be considered in detail. For example, Néel originally suggested a superparamagnetic relaxation of the spin lattices yielded by the lack of an internal structural perfection and (or) uncompensated surface spins [17] in antiferromagnetics. Some very recent studies [18–20] have been devoted to investigate the magnetic properties of  $\text{Co}_3\text{O}_4$  nanoparticles obtained by Quick Precipitation method [18] and by Continuous hydrothermal flow synthesis (CHFS) process [19]. A soft ferromagnetic material behavior was reported in [20] as a result of vibrating sample magnetometer (VSM) analysis. Also, some interesting magnetic properties at low temperature were observed for  $\text{Co}_3\text{O}_4$  nanoparticles in [19] as a result of magnetization versus temperature ( $M$  vs.  $T$ ) analyses.

In the present study, we have extended the study of  $\text{Co}_3\text{O}_4$  crystal to research the magnetic properties of  $\text{Co}_3\text{O}_4$  in a different morphology, including EPR measurements at high frequencies for investigations of anomalous magnetic properties of this antiferromagnetic crystal. Some deviations from the expected values of some magnetic properties have been determined and discussed by comparison with the relevant literature.

\* Corresponding author.

E-mail address: [muhammed.acikgoz@eng.bau.edu.tr](mailto:muhammed.acikgoz@eng.bau.edu.tr) (M. Açıkgöz).

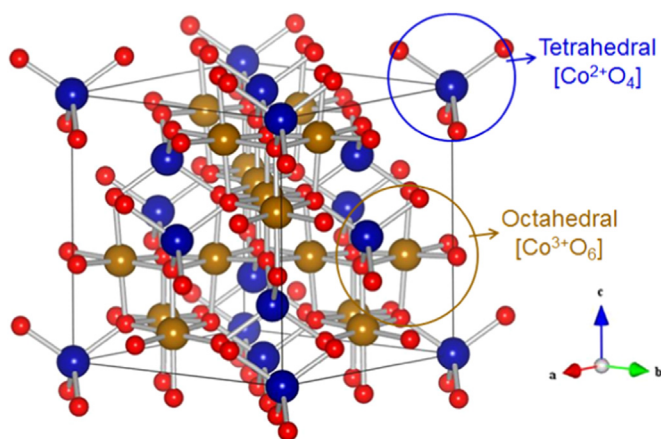


**Fig. 1.** Crystal structure and illustrations of the tetrahedral  $[\text{Co}^{2+}\text{O}_4]$  and octahedral  $[\text{Co}^{3+}\text{O}_6]$  coordinations in cubic  $\text{Co}_3\text{O}_4$  spinel structure.

## 2. Experimental details

The powder  $\text{Co}_3\text{O}_4$  (Puratronic 99.9985%, metal basis) obtained from Alfa Aesar GmbH was used as-received without any further modification. Standard powder x-ray diffraction at room temperature revealed the cubic spinel structure (space group:  $O_h^7\text{-Fd}3m$ ,  $a=8.10$  Å). A commercial superconducting quantum interference device (SQUID) magnetometer from Quantum Design was used to determine the susceptibility and magnetization of the samples within a temperature range  $1.5 \leq T \leq 400$  K. ESR measurements were performed with a Bruker ELEXSYS E500CW spectrometer at X-band and Q-band frequencies ( $\sim 9.5$  and 34 GHz, respectively) in temperature range  $4.2 \leq T \leq 300$  K. The spectrometer was equipped with an Oxford Instruments continuous He flow cryostat. ESR measurements at the temperatures between 300 and 500 K were performed at X-band frequencies using nitrogen gas-flow cryostat (Bruker). To improve the signal-to-noise ratio, one records the field derivative of the absorption  $dP_{\text{abs}}/dH$  by lock-in technique.

## 3. Results and discussion

Fig. 2 indicates the temperature dependences of the magnetic

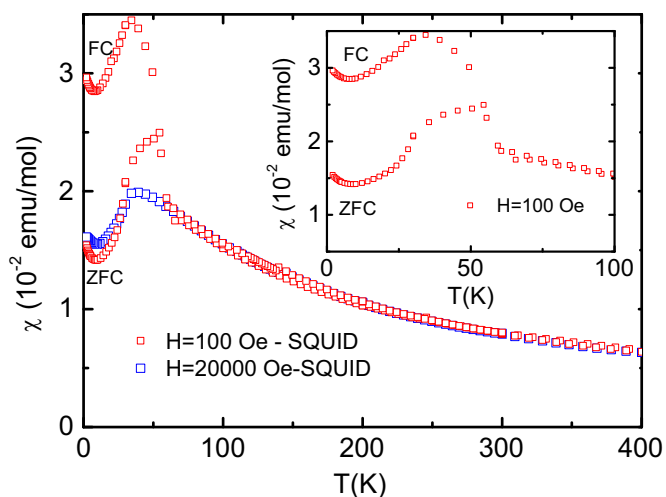


**Fig. 2.** Temperature dependences of the magnetic susceptibility of  $\text{Co}_3\text{O}_4$  polycrystal powder measured under application of magnetic field with intensities 100 Oe and 20 kOe. Inset: Detailed temperature behavior of the magnetic susceptibility of  $\text{Co}_3\text{O}_4$  in the temperature range of  $2 \text{ K} \leq T \leq 100 \text{ K}$  ( $H=100$  Oe).

susceptibility ( $\chi$ ) of  $\text{Co}_3\text{O}_4$  powder samples measured in zero-field-cooled (ZFC) and field-cooled (FC) regimes on applying measurement fields of two different intensities. For the zero-field-cooled (ZFC) mode, the sample was cooled from room temperature to 2 K and after making the certain stabilization of the temperature, magnetic fields of 100 Oe and 20 kOe were applied and the data were then recorded upon reaching the temperature of 400 K. While for FC mode, after cooling the sample under the same magnetic fields, the measurements were carried out and data was taken with increasing the temperature. As can be seen clearly from Fig. 2, an obvious bifurcation of the ZFC and FC curves appears at approximately 62 K. This behavior is very similar to that observed previously elsewhere for particles synthesized by CHFS process [19] and for nanoporous  $\text{Co}_3\text{O}_4$  nanorods synthesized in large quantity through the hydrothermal method [16]. After separation point along the lower temperature, FC magnetization exhibits a maximum at  $\sim 39$  K, which indicates antiferromagnetism of the  $\text{Co}_3\text{O}_4$  powder sample. The peak in the magnetic susceptibility ( $\chi$ ) in antiferromagnets generally takes place at a few percent higher temperature than the Néel temperature  $T_N$  is a well-known matter [21,22] and  $T_N=40$  K often quoted for bulk  $\text{Co}_3\text{O}_4$  in literature [2,23]. Hence, our result for  $T_N$  at  $\sim 39$  K agrees well with this statement. It is worthy to note that quite lower temperatures for both bifurcation of the ZFC and FC (at 44 K) and  $T_N$  ( $\sim 34$  K) were reported on the temperature dependence of magnetization ZFC and FC processes of  $\text{Co}_3\text{O}_4$  nanoparticles [18].

$1/\chi$  versus  $T$  plot for the powder  $\text{Co}_3\text{O}_4$  polycrystals is shown in Fig. 3. The data in this figure are fitted to the modified Curie-Weiss law  $\chi - \chi_0 = C/(T + \theta)$ , where  $\chi_0$  represents the temperature-independent orbital contribution and the diamagnetic contribution,  $C$  is the specific Curie constant and  $\theta$  is the Curie temperature. Usually  $\chi_0$  can be estimated using the high temperature data of the plot  $\chi$  vs.  $1/T$  in the limit of  $1/T$  goes to zero [15]. We have estimated  $\chi_0$  value from our  $\chi$  vs.  $T$  data up to 400 K in Fig. 3 as  $6.9 \times 10^{-3}$  emu/mol. Oe according to the similar procedure in [2,15]. From the fit of Fig. 3, the magnitude of  $C$  and negative  $\theta$  are determined as 0.35 emu K/mol Oe and 110 K, respectively. This is very consistent with the data observed in [19].

After obtaining the Curie constant ( $C$ ) from the inverse susceptibility, we then calculate the effective magnetic moment per ion using the expression  $C = \frac{N\mu^2}{3k_B}$  with  $\mu^2 = g^2J(J+1)\mu_B^2$ , where  $g$  is the Lande factor,  $J$  is the total angular momentum, and  $\mu_B$  is the Bohr magneton. For the magnitudes of  $g = 2.23$ , as observed from ESR measurements in the next section, expected spin contribution is as  $4.32\mu_B$  for  $\text{Co}^{2+}$  ( $S = 3/2$ ). Using the obtained value of  $C$ , it is

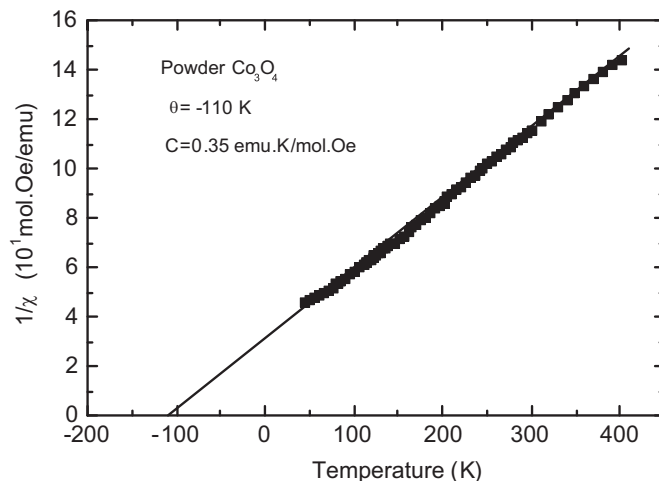


**Fig. 3.** The plot of  $1/\chi$  versus  $T$  for powder  $\text{Co}_3\text{O}_4$ . The solid line indicates the linear fit to the Curie-Weiss law.

Download English Version:

<https://daneshyari.com/en/article/1458741>

Download Persian Version:

<https://daneshyari.com/article/1458741>

[Daneshyari.com](https://daneshyari.com)